Metabolic Brain Disease (2019) 34:153–164
https://doi.org/10.1007/s11011-018-0331-2

ORIGINAL ARTICLE

Increased CD74 binding and EAE treatment efficacy of a modified DRα1 molecular construct

Roberto Meza-Romero[1,2,3] · Gil Benedek[1,2,3,4] · Grant Gerstner[1,3] · Gail Kent[1,3] · Ha Nguyen[1,3] · Halina Offner[1,3,5] · Arthur A. Vandenbark[1,2,3,6]

Received: 2 October 2018 / Accepted: 16 October 2018 / Published online: 23 October 2018

Abstract

Multiple sclerosis (MS) is a demyelinating and degenerative disease of the central nervous system (CNS) with a strong inflammatory component that affects more than 2 million people worldwide (and at least 400,000 in the United States). In MS, macrophage migration inhibitory factor (MIF) and D-dopachrome tautomerase (D-DT) enhance the inflammatory event as a result of their interaction with their cognate receptor CD74. Therefore, the search for new agents aimed at blocking this interaction is critical for therapeutic purposes and will be of paramount importance for the treatment of MS. DRα1-MOG-35-55 constructs have been demonstrated to be effective in the treatment of experimental autoimmune encephalomyelitis (EAE) a mouse model for MS. This effect is directly correlated with the binding to its cell surface receptor, CD74, apparently preventing or blocking the binding of two inflammatory factors, MIF and D-DT. Here we report that a single amino acid substitution (L50Q) in the DRα1 domain of the human and mouse DRα1-MOG-35-55 constructs (notated as DRhQ and DRmQ, respectively) possessed increased affinity for CD74, a greater capacity to block MIF binding, the ability to inhibit pERK1/2 signaling and increased therapeutic activity in mice with EAE. These data suggest that binding affinity for CD74 could serve as an in vitro indicator of biological potency of DRhQ and thus support its possible clinical utility as an effective therapy for MS and perhaps other diseases in which there is an inflammatory reaction driven by MIF and D-DT.

Keywords Multiple sclerosis · CD74 · EAE · MIF · D-dopachrome tautomerase · pERK1/2

✉ Arthur A. Vandenbark
vandenba@ohsu.edu

Gil Benedek
gilb@hadassah.org.il

[1] Neuroimmunology Research, Research Service R&D31, VA Portland Health Care System, 3710 SW US Veterans Hospital Rd, Portland, OR 97239, USA

[2] Department of Neurology UHS-46, Tykeson MS Research Laboratory, Oregon Health & Science University, 3181 SW Sam Jackson Park Rd, Portland, OR, USA

[3] Department of Neurology, Oregon Health & Science University, Portland, OR, USA

[4] Present address: Tissue Typing and Immunogenetics Laboratory, Hadassah Medical Center, Jerusalem, Israel

[5] Department of Anesthesiology and Perioperative Medicine, Oregon Health & Science University, Portland, OR, USA

[6] Department of Molecular Microbiology & Immunology, Oregon Health & Science University, Portland, OR, USA

Introduction

Multiple sclerosis (MS) is the most prevalent chronic inflammatory disease of both white and grey matter of the central nervous system (CNS), affecting more than 2 million people worldwide and at least 400,000 in the United States (Group 2017). Currently there is no cure for MS. Thus, MS patients have to rely on disease modifying therapies (DMT) (Wingerchuk and Carter 2014) in order to ameliorate some of the disease signs. About 15 disease-modifying medications are available for the relapsing and remitting form of MS (Reich et al. 2018). The inflammatory process in MS is mediated by autoimmune driven demyelination, often accompanied by neurodegenerative injuries (Frohman et al. 2006; Herrero-Herranz et al. 2008; Sospedra and Martin 2005; Steinman 1996). In both the animal model of MS, experimental autoimmune encephalomyelitis (EAE), and in MS subjects, multiple lines of evidence support the crucial role of autoreactive, myelin-specific, $CD4^+$ T cells in the autoimmune

disease process (Chitnis 2007; Herrero-Herranz et al. 2008; Steinman 1996; Zamvil and Steinman 1990). Key cytokines thought to drive the early inflammatory stage of MS to a chronic progressive phase are macrophage Migration Inhibitory Factor (MIF), the first described cytokine, and its ancestral functional homolog, D-dopachrome tautomerase (D-DT) (Benedek et al. 2017). MIF and D-DT levels are increased and have been implicated as markers of clinical worsening in MS and as a requirement for disease progression in EAE (Benedek et al. 2017; Meza-Romero et al. 2014; Niino et al. 2000; Powell et al. 2005).

Our laboratory designed a potent biological therapy called RTL1000 and a second-generation derivative, DRα1-human(h)MOG-35-55, that binds tightly to the MIF/D-DT receptor, CD74, and competitively inhibit MIF/D-DT binding and downstream signaling through phosphorylated extracellular signal-related kinases (p)ERK1/2 (Benedek et al. 2013, 2015; Vandenbark et al. 2003). RTL1000 and DRα1-hMOG-35-55 can treat mice with EAE after onset of clinical signs resulting in the inhibition of T cell and macrophage activation and migration into the CNS and reduced disease severity (Benedek et al. 2013; Vandenbark et al. 2003). RTL treatment was also found to enhance anti-inflammatory macrophage/microglia cell numbers, promote re-myelination and reduce the severity of acute and chronic EAE (Meza-Romero et al. 2014).

In this work we demonstrate: 1) an amino acid substitution of glutamine for leucine at position 50 (L50Q) of the DRα1-hMOG-35-55 construct (termed DRhQ) altered the affinity of the construct for CD74, with an 8 to 10-fold increase in binding capacity; 2) this substitution did not affect the structure of the molecule as evaluated by circular dichroism and antibody probing; 3) the increased binding affinity translated into a commensurate ability of DRhQ to competitively inhibit MIF binding to its cognate CD74 receptor; 4) treatment of EAE WT C57BL/6 mouse splenocytes with DRhQ reduced ERK1/2 phosphorylation in vitro to a background level; and 5) the L50Q substitution significantly enhanced the ability of the construct to treat ongoing clinical signs of severe EAE. These data suggest that binding affinity for CD74 could serve as an in vitro indicator of biological activity of DRhQ.

Material and methods

Fab, antibodies and other reagents

G4 is a human Fab reactive to the DRα1 domain derived from a human IgG library and was a kind donation from Dr. Yoram Reiter, Technion Israel. Anti-human MOG antibody was purchased from Santa Cruz Biotechnology. CHAPS, T20 and bovine serum albumin were purchased from Sigma-Aldrich. Anti-CD74 antibody was purchased from Everest Biotech. UltraPure™ TRIS was purchased from Invitrogen. Vector pET21d(+) was purchased from Novagen. BL21 (DE3) was purchased from New England Biolabs. IPTG was purchased from Inalco.

DRα1 constructs cloning, expression and purification

The DRα1 constructs purification has been reported (Vandenbark et al. 2003). Briefly, a synthetic DNA fragment containing a sequence encoding the human MOG-35-55 peptide, a flexible linker and the MHC Class II DRα1 domain from amino acid residues 15 through 97 and a similar synthetic DNA fragment containing the mutation L50Q in the DRα1 domain were cloned into the high level expression vector pET21d(+) (Novagen). These clones were transformed into *E. coli* strain BL21 (DE3) (New England Biolabs), plated onto LB-agar plates containing 50μg/ml of the antibiotic carbenicillin and incubated overnight at 37 °C. The next day three individual colonies from each clone were selected and grown in LB broth supplemented with the antibiotic to test IPTG-induced production of the protein of interest. After confirmation, a 100 ml overnight culture was prepared and used to inoculate a 4X1L flask with LB supplemented with the antibiotic. Induction of the target protein synthesis was performed with the addition at the logarithmic growth point of IPTG to a final concentration of 2 mM. The cultures were incubated for an additional 4 h at 37 °C, harvested by centrifugation and the bacterial paste was frozen at −80 °C until use. Pellets were resuspended in sonication buffer (50 mM Tris, 300 mM NaCl, 2 mM EDTA pH 8.0) and sonicated to disrupt the cells and release the inclusion bodies. The protein contained in these inclusion bodies were solubilized in a 20 mM ethanolamine, 6 M urea, pH 10 buffer overnight at 4 °C with gentle stirring. Purification was achieved by passing the solubilized protein through an anion exchange column and eluting the protein with a NaCl gradient in solubilization buffer. Fractions were collected and analyzed by SDS-PAGE. Those fractions containing the protein of interest were pooled together, dialyzed against 20 mM Tris, pH 8.5, concentrated to 5 mg/ml and flash frozen and then stored at −80 °C in 1 ml aliquots until use.

Amino acid sequence alignment

All the different Class II α1 domain sequences of interest were retrieved from the NCBI and aligned using BLAST Two or More sequences from BLAST website (NIH) and then optimized manually to show relevant regions.

Structural analysis of the proteins by circular dichroism

Proteins were thawed and analyzed by SDS-PAGE (data not shown) prior to testing for their secondary structures' content

by absorbance of far UV light (180-260 nm) using an AVIV spectrometer. Proteins were greater than 95% pure. One hundred microliters of each of the polypeptides were prepared in 20 mM Tris buffer pH 8.5 at 1 mg/ml concentration and placed in a CD cuvette. Protein were scanned for absorbance in the far UV spectrum from 180 nm to 260 nm through a 0.1 mm light pathlength taking measurements at 0.5 nm intervals. A sample containing only 20 mM Tris buffer was also scanned and the signal was subtracted from the protein readings. At least 3 scans were averaged for each protein and plotted as molar ellipticity.

Binding of DRα1 constructs to CD74 and competition assays

These experiments were performed by ELISA using Maxisorp plates (Nunc) as follows. Prior to the binding and competition experiments the proteins were labeled with Alexa Fluor 488 (Invitrogen) or biotin (Pierce Biotechnology) that targets lysine side chain primary amines. Unconjugated Alexa Fluor 488 or biotin were removed by size exclusion chromatography using a Superdex 75 10/300 column (GE Healthcare). For binding experiments, a recombinant human CD74 (rhCD74) construct was produced in our laboratory (data not shown) and the design, production and purification has already been described (Benedek et al. 2017). Plates were coated with rhCD74 (C27S) in TBS at a concentration of 0.1 μg/ml for 2 h at RT or overnight at 4 °C. After blocking with 5% BSA in TBS and 0.0125% Tween 20 (T20), DRα1-MOG constructs prepared in blocking buffer with 0.0125% T20 were captured for 3 h at room temperature followed by detection with streptavidin conjugated to horseradish peroxidase (HRP). Data were loaded onto Prism software and fitted to a one or two binding site equation in order to determine relative affinity. For competition experiments ELISA plates were coated with MIF at room temperature at a concentration of 0.5 μg/ml in TBS. Plates were then blocked overnight with 5% BSA in TBS and 0.0125% T20 followed by the addition of a competitive mix containing rhCD74 with serially diluted DRα1 constructs prepared in 5% BSA/TBS plus 0.0125% T20 for 1.5 h at 25 °C. Bound rhCD74 was detected with a monoclonal antibody that specifically recognizes human CD74 in a region away from the putative MIF/D-DT binding site. Absorbance at 450 nm was determined and data were analyzed with Prism, the parameters were calculated with the competition equation included in the software. For competition between DRα1-hMOG-35-55 and P2 peptide (see next section), mouse CD74 was immunoprecipitated from DR*1501 Tg mouse splenocytes and a competition experiment was set. 2.5 μl of P2 peptide were used with increasing concentrations of DRα1-hMOG-35-55 protein. Bound peptide was eluted from the immunoprecipitation with 2% SDS and analyzed in a 16.5% PAG Tris/Tricine. The gel was scanned for FITC and fluorescence was quantified by densitometry. P2 fluorescence vs. DRα1 competitor was plotted and data analyzed with Prism. The relative density values were fit to a One-binding site equation.

Mapping of the CD74-binding epitope on DRα1-hMOG-35-55

In earlier publications, we described an Fab that is able to bind the DRα1-MOG proteins and their parent molecule, RTL1000, with high affinity (Meza-Romero et al. 2014). However, its binding region on the DRα1 domain has not yet been determined. In order to map the epitope for the G4 Fab, a series of 7 overlapping N-terminus-FITC labeled peptides covering the full length of the DRα1 domain were synthesized. These peptides were tested for their ability to bind In1-immunoprecipitated mouse CD74 from splenocytes and immuno-adsorbed G4 to Protein L beads.

Immunoprecipitation and western blot experiments

After immuno-precipitation, individual peptides were analyzed in a binding experiment for 14–16 h in 0.1% CHAPS/TEN buffer (50 mM Tris, 2 mM EDTA, 150 mM NaCl, pH 7.4). Immune complexes were eluted with 50ul of 2% SDS/ESB (electrophoresis sample buffer) for 20 min and then analyzed by electrophoresis in a 10–20% SDS-PAGE under non-reducing conditions. After electrophoresis, the gel was scanned for FITC-labeled peptides. In a parallel experiment we used immunoprecipitated mouse H2M to test the binding of the peptide set. H2M molecules bind the Class II α1 domain but in different regions, therefore they should show a different selectivity for the α1 domain synthetic peptides during binding. We also tested the possibility of G4 and CD74 recognizing the same peptide set since we have found that G4 blocks binding of DRα1 constructs to rhCD74. In that regard, we bound G4 Fab to Protein L beads and then we applied either P2 or P7 peptides to the immune complexes. Bound material was eluted as described above, analyzed by electrophoresis and the gel scanned for FITC-labeled material. Western blot experiments were carried out using standard techniques of protein transfer to PVDF (pore size 0.1 μm), followed by blocking with 5% BSA in TBS and 0.05% T20.

ERK1/2 phosphorylation blockade

Two million splenocytes from EAE mice were treated in vitro at 37 °C with 20 mM Tris pH 8.5, 25μg of DRhQ or DRα1-hMOG-35-55 for 30 min. Cells were then spun down and lysed with RIPA buffer supplemented with protease and phosphate inhibitors. Cell lysis was allowed to proceed for 30 min in ice and the debris containing nuclei and organelles removed by centrifugation at

14,000 rpm at 4 °C for 10 min. Supernatants were collected and subjected to SDS-PAGE in 10–20% gradient gels under reducing conditions. After electrophoresis, proteins were transferred to PVD membrane and the membrane was probed first for p-ERK1/2, stripped and then probed with anti-total ERK1/2 antibody.

EAE induction and treatment

C57BL/6 WT male mice between 8 and 12wks of age were purchased from the Jackson Laboratory. All procedures were approved and performed according to federal, state, and institutional guidelines. Mice were immunized subcutaneously at four sites on the flanks to distribute 0.2 ml of an emulsion of 200 μg mouse MOG-35-55 peptide and complete Freund's adjuvant containing 400 μg of heat-killed Mycobacterium tuberculosis H37RA (Difco) (Meza-Romero et al. 2014). In addition, mice were injected intraperitoneally with Pertussis toxin (Ptx) from List Biological Laboratories on days 0 and 2 post-immunization (75 and 200 ng per mouse, respectively). DRα1-hMOG-35-55, DRhQ, DRα1-mMOG-35-55 and DRmQ proteins (100 μg in 0.1 ml) were injected s.c. daily for 5 days beginning at an EAE score of ≥2.0 and the mice were scored for clinical signs of EAE graded on a six-point scale of combined hindlimb and forelimb paralysis scores as described before (Meza-Romero et al. 2014). Mean EAE scores and SDs for mouse groups were calculated for each day from day 8 through day 27 post-immunization and summed for each mouse by numerically integrating the EAE score curve over the entire experiment (CDI, represents total disease load).

Data analysis

Statistical analyses comparing EAE severity data and equation fitting data for binding and competition results were computed using a Prism software package (GraphPad).

Results

Protein production and characterization

The production of DRα1-hMOG-35-55, DRα1-mMOG-35-55, DRhQ and DRmQ proteins were comparable, indicating that the L50Q substitution did not affect the transcription and the expression rate (data not shown). The protein yield was consistently ~90 to 100 mg/l of LB broth. Fab G4 was used to detect the purified proteins. In previous studies, it was shown that Fab G4 detected the DRα1 domain in different contexts, including as a stand-alone domain, as part of larger constructs (like the ones described here) or as part of a two-domain recombinant protein (like RTL1000).

Amino acid sequences alignment

An analysis of the alignment of several human Class II α1 domains revealed a unique characteristic of the DRα1 domain not shared with other human or mouse class II (Fig. 1). This unique feature shows a glutamine (Q) residue at position 18 in most of the sequences used in the alignment (Q18, see arrow in Fig. 1). The DRα1 domain, however, has a leucine (L) at position 18. It is noteworthy that along with the other peptide-presenting Class II domains, this Q18 residue is also conserved among the non-antigen presenting proteins DMα1 and DOα1. In all the analyzed Class II α1 domain primary sequences and the crystal structures deposited in the Protein Data Blank (PDB), this region localizes in the loop between β-strand 1 and β-strand 2 at the N-terminus of the polypeptide pointing outwards of the bulk of the molecule.

Binding assays of RTL's from human and mouse origin

In order to explore the functional role of L18 vs. Q18, we first ran binding assays in ELISA experiments using several previously constructed RTLs from mouse and human origin. Figure 2a shows that those polypeptides which have Q18 [DP2, DP4, and mouse derived polypeptide RTL 551 (IAb)] displayed greater binding activity to rhCD74 in ELISA assays than constructs using >L18. This observation prompted us to produce these mutant polypeptides (sequences shown in Fig. 2b) to investigate whether L18 vs. Q18 (position 50 in the DRα1-MOG-35-55 constructs) might have different binding affinities for the CD74 receptor.

Evaluation of the DRα1-MOG-35-55 constructs using Fab G4 characterization and circular dichroism

After purification, the constructs were first tested for structural integrity. We used human Fab G4 (that recognizes the DRα1 domain) as a tool to find out whether the L50Q substitution affected the immunological recognition of the DRα1 constructs. The Fab G4 cross-reacted with the DRhQ mutant in the same manner as it did with the DRα1-hMOG-35-55 as well as the DRα1-mMOG-35-55 (Fig. 3a). In order to compare the secondary structure content of the DRhQ and DRα1-MOG-35-55 proteins side by side we carried out far UV scanning of the protein in a circular dichroism spectrometer. (Figure 3b). We reported in previous studies that DRα1-hMOG-35-55 contains a significant amount of alpha-helix and beta sheet secondary structures (Meza-Romero et al. 2014). All the molecules showed a high positive absorbance at 190 nm, the main feature indicative of an α-helix element, and a negative absorbance at 215 nm indicating the presence of β-sheet secondary structure. Overall, these results show that the three proteins are structurally similar suggesting that the replacement of a Leucine (L) for a Glutamine (Q) in the β-

Fig. 1 Class II α1 domain alignment showing a Q residue at position 18 (indicated by an arrow). The amino acid residue Q18 (nomenclature taken from the sequences reported in protein data bank) is highly conserved among the class II α chains, except with DRα1. Here position 18 was changed from L to Q by site-directed mutagenesis

```
                10        20        30        40        50        60
DM1   WPDDLQNHTF LHTV-YCQDG SPSVGLSEAY DEDQLFFFDF SQNTRVPRLP EFADWAQEQG
DO1   AGATKADHMG SYGPAFYQSY GASGQFTHEF DEEQLFSVDL KKSEAVWRLP EFGDFARFDP
DQ1   GEDIVADHVA SCGVNLYQFY GPSGQYTHEF DGDEQFYVDL ERKETAWRWP EFSKFGGFDP
DQ2   GEDIVADHVA SYGVNFYQSH GPSGQYTHEF DGDEEFYVDL ETKETVWQLP MFSKFISFDP
DP4   RRVIKADHVS TYAA-FVQTH RPTGEFMFEF DEDEMFYVDL DKKETVWHLE EFGQAFSFEA
DP2   AGAIKADHVS TYAA-FVQTH RPTGEFMFEF DEDEMFYVDL DKKETVWHLE EFGQAFSFEA
DR1   SWAIKEEHVI IQA-EFYLNP DQSGEFMFDF DGDEIFHVDM AKKETVWRLE EFGRFASFEA
IAk   EDDIEADHVG SYGITVYQSP GDIGQYTFEF DGDELFYVDL DKKETVWMLP EFAQLRRFEP
IAd   EDDIEADHVG FYGTTVYQSP GDIGQYTHEF DGDELFYVDL DKKKTVWRLP EFGQLILFEP
IAb   EDDIEADHVG TYGTSVYQSP GDIGQYTFEF DGDELFYVDL DKKKTVWRLP EFGQLASFDP
IAf   EDDIEADHVG FYGISVYQSP GDIGQYTFEF DGDEWFYVDL DKKETVWRLP EFGQLTSFDP
IAu   EDDIEADHVG SYGIVVYQSP GDIGQYTFEF DGDELFYVDL DKKETIWMLP EFAQLRSFDP
IAq   EDDIEADHVG SYGIVVYQSP GDIGQYTHEF DGDEWFYVDL DKKETVWMLP EFGQLTSFDP
```

sheet platform of the constructs alters only minimally the α-helix content but does not alter the amount of β-sheet structure at the bottom of the molecule.

CD74-binding site on DRα1 maps to the N-terminus

Seven overlapping peptides spanning the whole length of the DRα1 protein were designed (Fig. 4a). These peptides contained a FITC moiety at the N-terminus of the amino acid sequence in order to be detected by fluorescence scanning. Of these, P1 had to be modified due to a solubility issue of the full length peptide and a second peptide (P6) could not be synthesized. These peptides were used, individually and as a pool, to bind immuno-precipitated CD74 from mouse splenocytes. As a first approach a cocktail of all peptides were added simultaneously to Protein A/G beads containing ln1-immunoprecipitated CD74. As is shown in Fig. 4b only 2 peptides, P2, and P5 to a minor extent, bound to immunoprecipitated mouse CD74. To confirm this we ran an experiment in which individual peptides were added to the Protein A/G-ln1-CD74 complexes under the same conditions. As shown in the same Fig. 4b, only P2 and P5 peptides bound clearly to mouse CD74. P2 exhibited stronger binding, while P5 had lower affinity. In order to test the usefulness of this strategy we ran an experiment with immuno-precipitated H2M. We hypothesized that a different peptide (or set of peptides) would bind to H2M. As seen in Fig. 4c**,** an entirely different set of the overlapping peptides bound to this protein, validating the results of the previous experiment. This later experiment showed that P7 peptide strongly bound immunoprecipitated H2M and to a minor extent P4. This result is consistent with the crystal structure of the DR/DM complex published recently (Pos et al. 2012). The interface of these two molecules is dominated by the alpha chains of DM and DR. DM binds to a lateral surface of the DRα1 domain away from the N-terminus of the DRα1 region and close to the peptide binding groove without contacting the DRβ1 domain. Overall, this approach validated the designed strategy to investigate this paradigm.

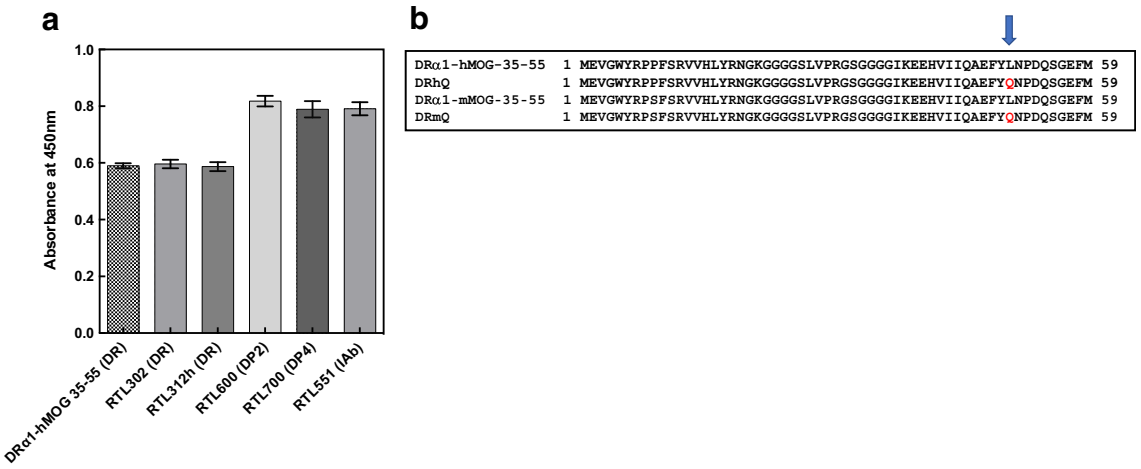

Fig. 2 Binding of DRα1-hMOG-35-55, human MHC Class II DR-derived RTL302, human Class II DR-derived RTL312, human Class II-derived DP2- and DP4-derived constructs to rhCD74(C27S). In addition, we tested the binding of a mouse MHC Class II-derived RTL551 to coated rhCD74(C27S). Binding experiment was carried out using equimolar concentration (250 nm) of each protein ligand (Fig. 2a). Alignment showing the final amino acid sequence of the Q mutants compared to the WT versions created in this work. In addition to the DRα1-hMOG-35-55 and the DRhQ we synthesized the DRα1-mMOG-35-55 and DRmQ. The arrow indicates the positions of the mutagenesis (Fig. 2b)

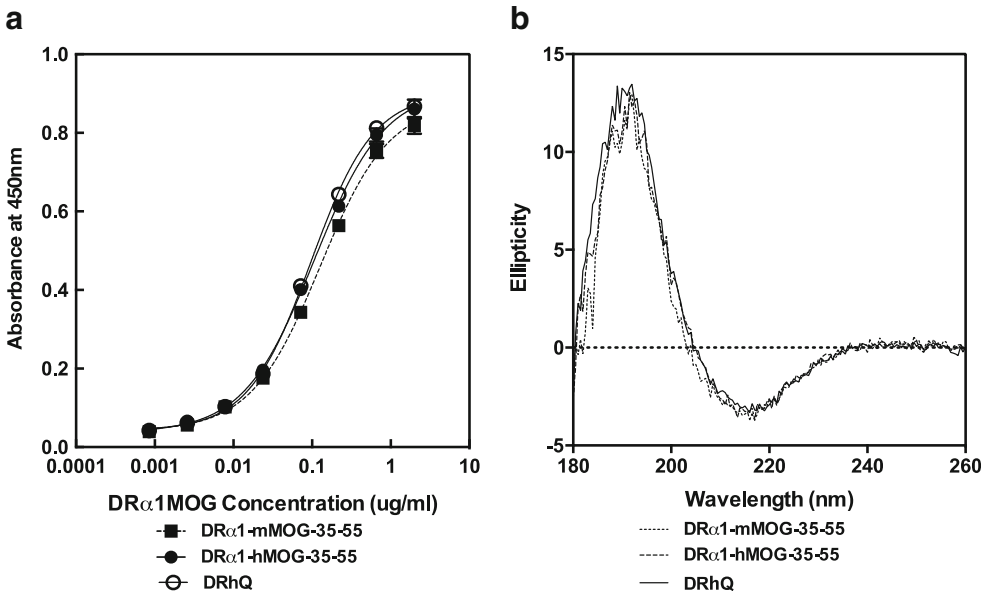

Fig. 3 DRα1-derived constructs DRα1-hMOG-35-55, DRα1-mMOG-35-55 and DRhQ were probed with the Fab G4 (Fig. 3a) in order to evaluate immunological differences among them (the characterization of the DRmQ is not shown). Circular dichroism was used to evaluate differences in secondary structure content as described before (Fig. 3b)

P2 binds the G4 Fab, binds to IP CD74 and competes with DRα1-hMOG-35-55 to bind its CD74 receptor

In previous publications, we have shown that the G4 Fab was effective to block DRα1 constructs binding to CD74 on the cell surface of mouse and human CD11b cells (Meza-Romero et al. 2014). Therefore, we aimed to find out whether P2 also interacted with Protein L bound G4 Fab and compare the binding to immunoprecipitated CD74. Potentially, the P7 would not bind to G4 or CD74 in agreement with the previous experiment

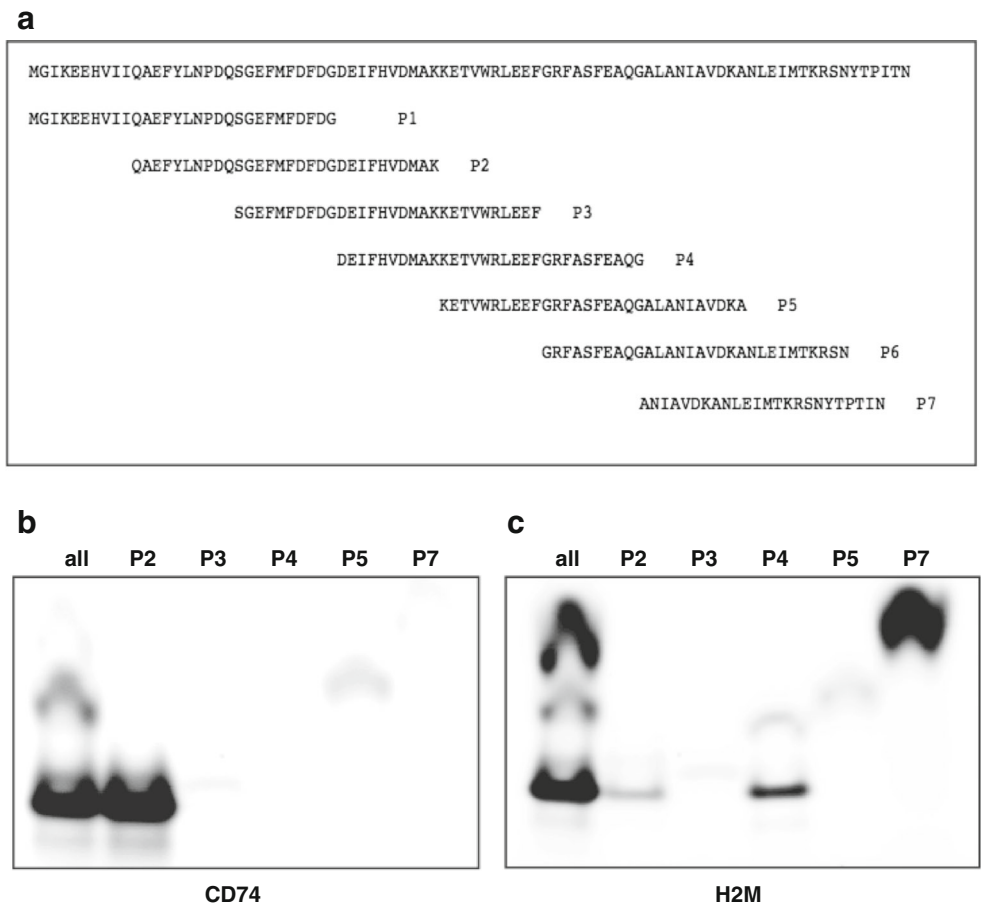

Fig. 4 Strategy was designed to locate the DRα1 binding site for CD74. Overlapping peptides used in this experiment to identify the binding region to CD74 (Fig. 4a). Mouse CD74 or mouse H2M were immunoprecipitated with specific monoclonal antibodies adsorbed to Protein A/G beads and then a pool of the overlapping peptides or individual peptides were added. Immune complexes were washed extensively and bound peptides were eluted with electrophoresis sample buffer containing 1% SDS. Eluted material was analyzed by electrophoresis by SDS-peptide gels in Tris-Tricine. Gels were then scanned for the fluorophore in a BioRad Molecular Imager FX (Fig. 4b, c)

described in Fig. 4. As expected, only the P2 peptide was able to bind G4, demonstrating that G4 and CD74 have the same binding site on DRα1 polypeptides (Fig. 5a). Figure 5b shows a schematic view of the DRα1 domain (colored in cyan) with the P2 peptide location (colored in green). To confirm that the P2 peptide was associated with the interface to bind CD74 we ran an experiment to find out whether DRα1-hMOG-35-55 and P2 peptide compete with each other to bind mCD74. The results showed that DRα1-hMOG-35-55 was able to outcompete the binding of the FITC-labeled P2 peptide to immunoprecipitated CD74 with a relative affinity (K_D) of 750 nM (Fig. 5c).

DRα1-MOG-35-55 and DRhQ binding to rhCD74 and ELISA competition assays

DRα1-MOGs, including DRα1-hMOG-35-55, DRhQ, DRα1-mMOG-35-55 and DRmQ were evaluated for binding to their receptor. A recombinant human CD74(C27S) produced in our laboratory was coated onto the ELISA plate and then, following blocking, DRα1 constructs were captured for 1 to 1.5 h at RT and detected with an anti-MOG antibody. The results were entered into the Prism software and the K_D was calculated after fitting the curve to a One-site specific binding equation. As shown in Fig. 6a and in Table 1 these results clearly indicate that the replacement of leucine at position 50 of the DRα1 constructs (or position 18 in the alignment, or 14 in the original PDB sequences) for a glutamine residue clearly increased the binding capacity of the mutant proteins. We found that the DRhQ mutant bound with 8 to 10-fold higher affinity to the receptor when compared to the counterpart wild type version of the constructs. (see Table 1 with K_D). This confirms that the region containing the L50 is very likely a part of the binding site of DRα constructs to CD74 as suggested by the docking model of the DRα/CD74 interaction (Meza-Romero et al. 2016b; Wingerchuk and Carter 2014) and the experiments with the P2 peptide (see previous section). Competition assays were consistent with the direct binding results (Fig. 6b). In the competition experiments the DRhQ showed greater ability, 8 to 10-fold, to outcompete MIF for its binding to CD74 than the DRα1-hMOG-35-55 (DRhQ $IC_{50} = 0.28$uM vs DRα1-hMOG-35-55 $IC_{50} = 1.6$uM) arguing in favor of a more direct role that this region contributes to the binding interaction. On the other hand, DRα1-mMOG-35-55 and its derivative DRmQ showed no significant differences between them and displayed an intermediate competitive activity when compared to DRhQ.

EAE treatment

We then sought to test these polypeptides for their ability to treat EAE mice**.** As shown in Fig. 7a, treatment of male C57BL/6 mice with the DRhQ construct significantly reduced the severity of ongoing EAE compared with the native L50 containing DRα1-hMOG-35-55 construct. In contrast, treatment with the DRmQ, which did not differ in its ability to

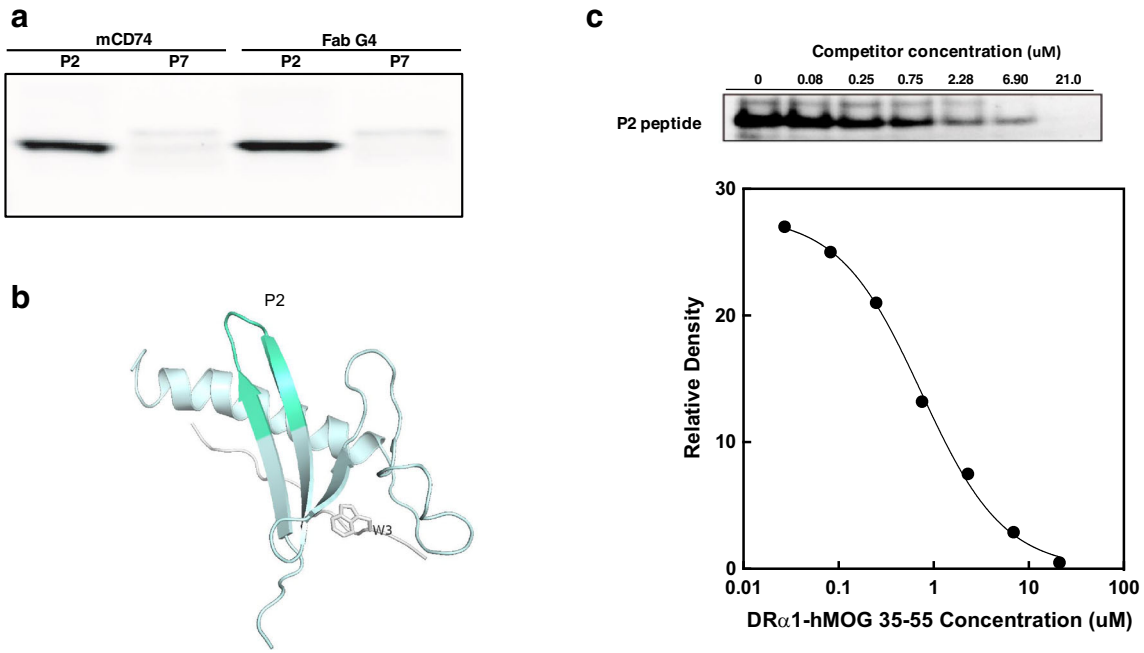

Fig. 5 Two of the overlapping peptides were tested individually for their ability to bind immunoprecipitated mouse CD74 or Fab G4 adsorbed to Protein A/G beads and Protein L beads, respectively. Only P2 was able to bind rhCD74 and Fab G4. P7 was unable to bind to any of the targets (Fig. 5a). Graphic representation of the P2 location in the DRα1 domain structure. A schematic view of the DRα1 domain (colored in cyan) with the P2 peptide location (colored in green) (Fig. 5b). Competition experiment showed that DRα1-hMOG-35-55 was able to outcompete the binding of the FITC-labeled P2 peptide to immunoprecipitated CD74 with a relative affinity (K_D) of 750 nM (Fig. 5c)

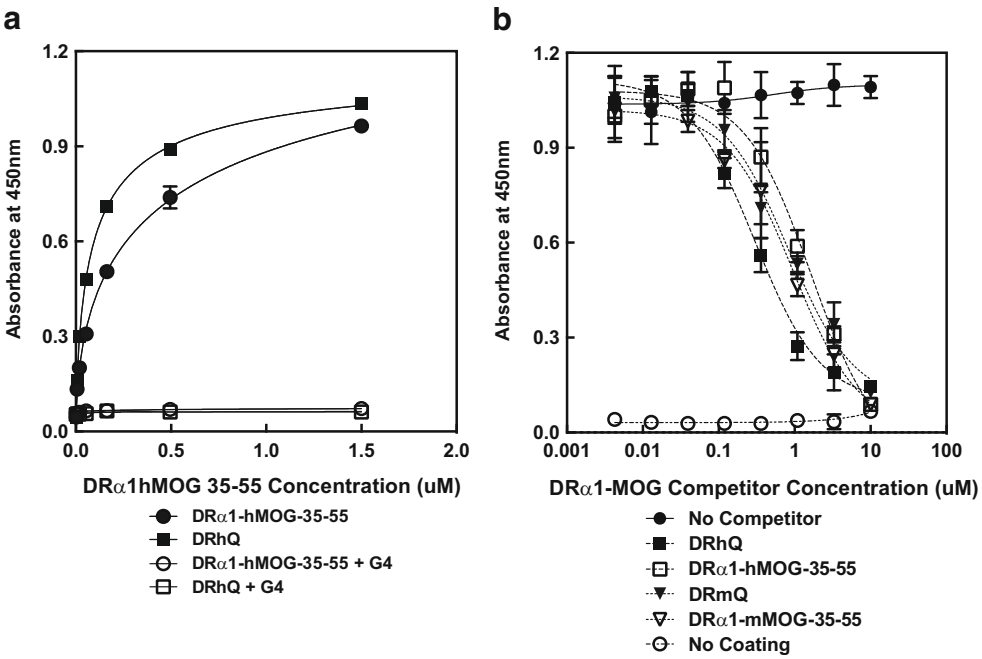

Fig. 6 Constructs DRα1-hMOG-35-55 and the DRhQ (Fig. 6a) were assessed for direct binding to rhCD74 onto ELISA plates by direct binding assay with or without G4 Fab during the binding. The K_D calculated polypeptides were 0.65uM for the DRα1-hMOG-35-55 and 0.089 for the DRhQ. In a competitive experiment DRhQ showed higher activity against rhMIF to bind CD74 compared to the DRα1-hMOG 35–55 (Fig. 6b) and Table 1

block MIF binding to CD74 (see above), did not differ in its treatment effect on EAE compared with the L50 containing DRα1-mMOG-35-55 construct (Fig. 7b).

DRhQ blocks ERK1/2 phosphorylation in mouse splenocytes

Studies have shown that MIF is the main pro-inflammatory cytokine driving the ERK1/2 phosphorylation through the interaction with CD74/CD44 on the cell surface (Leng et al. 2003). We therefore determined the level of ERK1/2 phosphorylation in non-treated EAE mice. Splenocytes harvested from EAE mice showed upregulated levels of p-ERK1/2 indicating an ongoing active signaling cascade associated with the inflammatory process. Upon treatment with the DRhQ constructs in vitro the phosphorylation level was downregulated after 30 min incubation at 37 °C. This strongly suggests that treating splenocytes from an animal with an ongoing inflammatory reaction with the constructs resulted in down regulation of ERK1/2 phosphorylation (Fig. 8).

Discussion

Our laboratory has been working on the design, development and characterization of novel experimental drugs aimed at treating MS subjects. RTL1000, a drug that has been used in the treatment of EAE, and the second-generation DRα1-hMOG-35-55 construct derived from it, have shown promise as novel therapeutic options to treat EAE and potentially MS (Benedek et al. 2015; Meza-Romero et al. 2014). Previous studies found that these constructs bind to the cell surface of macrophages/monocytes with high specificity and in a saturable pattern suggesting the presence of a receptor (Vandenbark et al. 2013). The binding to the cell surface receptor was correlated with their ability to alleviate EAE symptoms in

Table 1 Calculated binding affinities of DRα1-hMOG-35-55 and DRhQ for rhCD74(C27S)

Binding affinities (uM) for DRα1-hMOG-35-55 and DRhQ for CD74				
	DRhQ	DRα1-hMOG-35-55		
K_D	0.09109	0.7015		
95% CI	0.07146 to 0.1161	0.1304 to 1.774		
R square	0.999	0.996		
Competition of DRα1-MOG constructs vs MIF to bind CD74				
	DRhQ	DRα1-hMOG-35-55	DRmQ	DRα1-mMOG-35-55
IC50	0.2978	1.639	0.8279	0.9369
95% CI	0.1821 to 0.4870	0.9047 to 2.968	0.4599 to 1.490	0.4783 to 1.835
R square	0.9691	0.9601	0.9658	0.9461

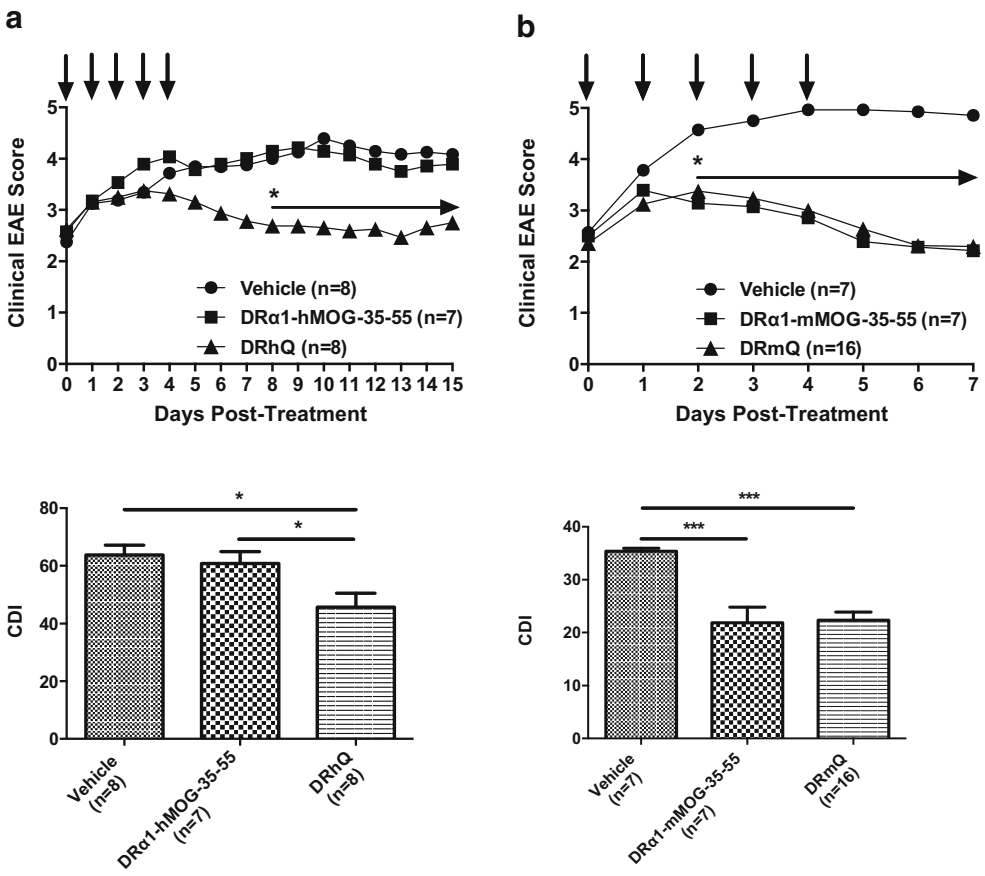

Fig. 7 C57BL/6 WT male mice between 8 and 12wks of age were purchased from the Jackson Laboratory and immunized as described in Material and Methods. DRα1-hMOG-35-55 and DRhQ (Fig. 7a) or DRα1-mMOG-35-55 and DRmQ (Fig. 7b) proteins (100 μg in 0.1 ml) was injected s.c. daily for 5 days beginning at an EAE score of ≥2.0 and the mice were scored for clinical signs of EAE. Mean EAE scores and SDs for mouse groups were calculated for each day from day 8 through day 27 post-immunization and summed for each mouse by numerically integrating the EAE score curve over the entire experiment (CDI, represents total disease load)

experimental animals (Benedek et al. 2017). We found that these two experimental drugs bound to the cell surface receptor CD74 (Vandenbark et al. 2013) present in antigen presenting cells like macrophages, monocytes and B cells. The CD74 transmembrane protein has also been shown to be a receptor for MIF and D-DT (Leng et al. 2003).

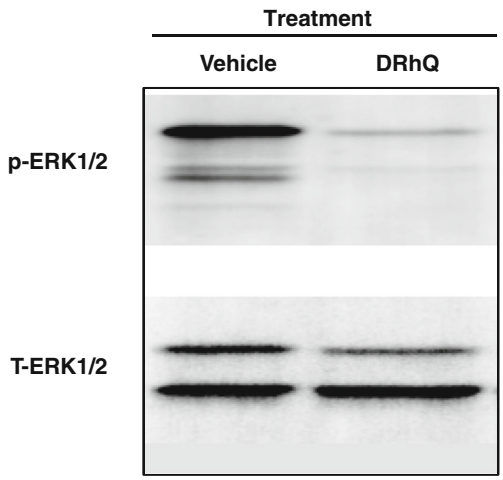

Fig. 8 ERK1/2 phosphorylation assay. 2 million cells from EAE mice were treated with vehicle, DRhQ or DRα1-hMOG-35-55 for 30 min and then cells were lysed in the presence of protease and phosphatase inhibitor. Supernatants were analyzed by electrophoresis and WB to evaluate P-ERK1/2 and total ERK1/2. DRα1-hMOG-35-55 and DRhQ were able to downregulate ERK1/2 phosphorylation in vitro

An alignment of the available human and mouse α1 domain amino acid sequences showed a Q residue at position 18 (position 14 in the crystal structure numbering) in most of them. The fact that this residue is present in human antigen-presenting (DP and DQ alleles) and non-antigen presenting regulatory (DM and DO) polypeptides, and in those from mice, argues in favor of a relevant role in the biological activity of these molecules. This Q residue is naturally substituted for a Leucine in the DRα1 domain (see Fig. 1). Experimental evidence suggests that this region could be a potential extra binding site for CD74 (Karp et al. 1992, 1990; Kim et al. 1994), in addition to the CLIP sequence (Jasanoff et al. 1999). As a first approach, we evaluated the binding properties of constructs that are derived from these Class II alleles and compared them to the binding parameters of DRα1 polypeptides. Surprisingly, the results of this experiment indicated that the constructs natively displaying the Q in the α1 domain indeed showed higher affinity for CD74 in direct binding assays by ELISA (Fig. 2a). Interestingly, in the crystal structures of several human and mouse Class II molecules deposited in the Protein Data Bank, the Q amino acid residue locates at the end of the β-strand 1 in the loop between the β-strand 1 and the β-strand 2 at the N-terminus of the domain (Fig. 9a, b). In fact, this loop has been

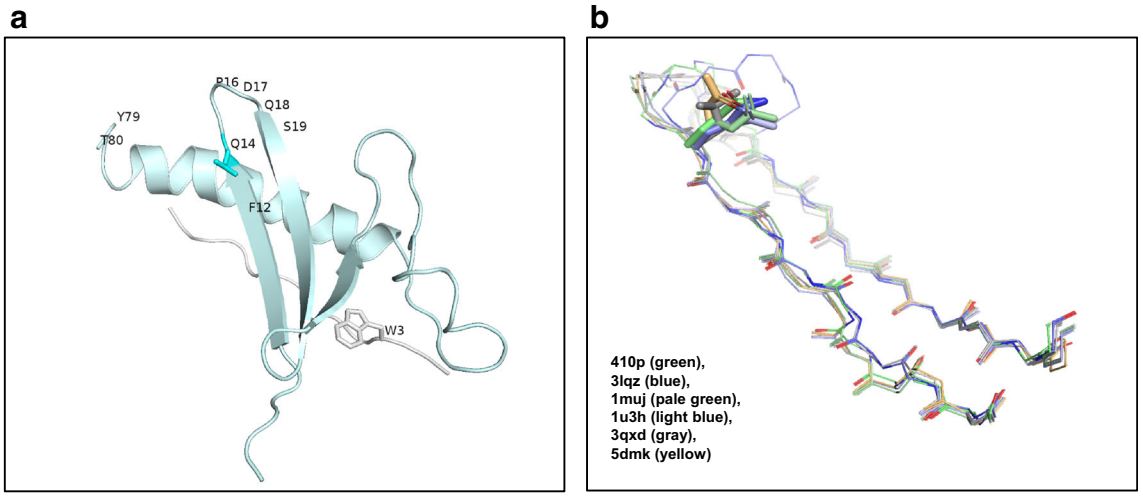

Fig. 9 Ribbon-rendered structure model. Shows the position of relevant amino acid residues in the DRhQ construct described in this work and that were shown by the docking model to contact CD74. The Q is highlighted with a stick-drawn side chain at position 14. The antigenic MOG peptide is shown in white and the side chain for W3 in the MOG peptide is displayed (Fig. 9a**)**. Several α1 domains from molecules described in Fig. 1 were recovered from the Protein Data Bank and their β-strand 1-loop- β-strand 2 regions aligned using PyMOL (Schrodinger, Portland OR). Position 14 has been highlighted as sticks. The PDB entries are shown in the inset (Fig. 9b**)**. Note: the amino acid residues numbering in the Fig. 1 differs from the numbering in the crystal structures: Q18 in Fig. 1 corresponds to amino acid residue 14 in most of the crystal structures and is located at the end of the β-strand 1 of the domain

implicated in the binding of the TSST-1 toxin to the a1 domain of class II (Karp et al. 1990; Kim et al. 1994) and the association between Class II and the invariant chain (Ii, CD74) prevents binding of TSST to Class II (Karp et al. 1992) suggesting a potential shared or overlapping epitope. Using a protein-protein docking algorithm, our laboratory predicted the existence of an interface between CD74 and DRα1-hMOG-35-55 (Meza-Romero et al. 2016b; Wingerchuk and Carter 2014) and defined the amino acid residues F48, L50, P52, D53 and S55 in the construct (F12, L14, P16, D17 and S19, in Fig. 9a) as important components of this interface. We therefore introduced the Q mutation into the DRα1-hMOG-35-55 and the DRα1-mMOG-35-55 to create the DRhQ and the DRmQ variants, respectively. From the immunological and biophysical standpoints, these novel mutants are indistinguishable from their parent molecules. Both proteins show the same level and quality of cross-reaction to the Fab G4, suggesting that the epitope has not been structurally modified (Fig. 3a). Likewise, both constructs show identical profiles by circular dichroism spectrometry indicating that the secondary structure has been preserved in the mutants' DRhQ (Fig. 3b) and DRmQ (not shown). Earlier experimental studies suggested that in addition to DRα1-MOG-35-55 (Benedek et al. 2013), RTL1000 was also able to bind to and block MIF binding to CD74 (Benedek et al. 2017). By using a set of overlapping peptides spanning the DRα1 domain amino acid sequence the major binding site was narrowed down to the N-terminus of the DRα1 domain (Fig. 4a, b) as predicted by the docking algorithm (Meza-Romero et al. 2016a; b). All these amino acid residues make up the core of the P2 peptide that was shown to bind to immunoprecipitated mouse CD74 and to Fab G4 (Fig. 5a). In addition, DRα1-hMOG-35-55 outcompeted the P2 peptide to bind to immunopurified mouse CD74 (Fig. 5c) indicating that both ligands bind to the receptor in the same region. A close inspection of crystal structures of several mouse and human MHC Class II molecules showed that these residues are located in the loop between the β1 and β2 strands at the N-terminus of the α1 domain. According to our docking model, the residues within this loop make close contact with residues on CD74 (Fig. 9a). We also tested this novel variant for its binding to a recombinant version of human CD74 and its activity to prevent or outcompete MIF from binding to their receptor. Our results indicate that the Q-harboring variant showed a $\mathbf{K_D}$ 8–10-fold higher affinity for CD74 in direct binding ELISA assays, in sharp contrast to the parent molecule, suggesting that the Q at this position favorably influenced the interaction (Fig. 6a**,** Table 1). Accordingly, DRhQ showed more competitive activity versus MIF to bind the CD74 receptor with an 8 to 10-fold higher $\mathbf{IC_{50}}$**(see** Fig. 6b, Table 1**)**. It is interesting to note that this higher affinity evaluated by direct binding and by competition experiments was reflected in the potency of the drug to treat EAE in experimental animals. As shown in Fig. 7**,** these constructs were able to significantly reduce the disease scores in mice compared to a lack of a treatment effect with DRα1-hMOG-35-55 with this disease severity. In previous work we have shown that with a lower disease severity, DRα1-hMOG-35-55 is able to stop disease progression in C57BL/6 (unpublished) and DR1 Tg mice (Vandenbark et al. 2003). Previous work has shown that MIF engagement of the CD74 receptor and its co-receptor CD44 at the cell surface initiates a signaling cascade leading to the phosphorylation of ERK1/2 and ultimately to the expression of

inflammatory genes (Benedek et al. 2013; Leng et al. 2003). Our experiments demonstrate that splenocytes harvested from EAE mice showed upregulated levels of p-ERK1/2 indicating an ongoing active signaling cascade associated with the inflammatory process and that this phosphorylation of ERK1/2 can be down regulated by DRhQ treatment in vitro (Fig. 8).

In conclusion, we show that a substitution of Q for L at position 18 in the first DRα1 loop region (position 14 in Fig. 9a, b) alters its affinity for CD74 with an 8 to 10-fold increase in binding capacity. We also show that this increase in binding activity translates into a greater ability of DRhQ to compete with MIF to bind its cognate receptor with the same 8 to 10-fold magnitude and that this renders the molecule capable of blocking MIF-induced signaling through pERK. This increased binding capacity translates into a more effective treatment of EAE in mice. These data suggest that binding affinity for CD74 could serve as an in vitro indicator of biological potency of DRhQ and thus support its possible clinical utility as an effective therapy for MS and perhaps other diseases in which there is an inflammatory reaction driven by MIF and D-DT.

Acknowledgments This work was supported by the National Institute of Allergy and Infectious Diseases award R42AI122574 (AAV), National Institute Of Neurological Disorders And Stroke R01NS080890 and the American Heart Association 17GRNT33220001 (HO), and the Department of Veterans Affairs, Veterans Health Administration, Office of Research and Development, Biomedical Laboratory Research and Development Merit Review Award 2I01 BX000226 (AAV). The contents do not represent the views of the Department of Veterans Affairs or the United States Government. We thank Dr. Yoram Reiter and the Technion Israel for the donation of G4.

Funding This work was funded by the National Institute of Allergy and Infectious Diseases award R42AI122574 (AAV), National Institute Of Neurological Disorders And Stroke R01NS080890 and the American Heart Association 17GRNT33220001 (HO), and the Department of Veterans Affairs, Veterans Health Administration, Office of Research and Development, Biomedical Laboratory Research and Development Merit Review. Award 2I01 BX000226 (AAV). The contents do not represent the views of the Department of Veterans Affairs or the United States Government.

Compliance with ethical standards

Conflict of interest Drs. Vandenbark, Offner, Benedek, Meza-Romero and OHSU have a significant financial interest in Artielle ImmunoTherapeutics, Inc., a company that may have a commercial interest in the results of this research and technology. This potential conflict of interest has been reviewed and managed by the OHSU and VA Portland Health Care System Conflict of Interest in Research Committees. The other authors (Grant Gerstner, Gail Kent, Ha Nguyen) declare no conflicts of interest.

Ethical approval All applicable international, national, and/or institutional guidelines for the care and use of animals were followed. All procedures performed in studies involving animals were in accordance with the ethical standards of the institution or practice at which the studies were conducted. This article does not contain any studies with human participants performed by any of the authors.

References

Benedek G et al (2013) Partial MHC class II constructs inhibit MIF/CD74 binding and downstream effects. Eur J Immunol 43:1309–1321. https://doi.org/10.1002/eji.201243162

Benedek G, Meza-Romero R, Jordan K, Keenlyside L, Offner H, Vandenbark AA (2015) HLA-DRalpha1-mMOG-35-55 treatment of experimental autoimmune encephalomyelitis reduces CNS inflammation, enhances M2 macrophage frequency, and promotes neuroprotection. J Neuroinflammation 12:123. https://doi.org/10.1186/s12974-015-0342-4

Benedek G et al (2017) MIF and D-DT are potential disease severity modifiers in male MS subjects. Proc Natl Acad Sci U S A 114: E8421–E8429. https://doi.org/10.1073/pnas.1712288114

Chitnis T (2007) The role of CD4 T cells in the pathogenesis of multiple sclerosis. Int Rev Neurobiol 79:43–72. https://doi.org/10.1016/S0074-7742(07)79003-7

Frohman EM, Racke MK, Raine CS (2006) Multiple sclerosis–the plaque and its pathogenesis. N Engl J Med 354:942–955. https://doi.org/10.1056/NEJMra052130

Group GBDNDC (2017) Global, regional, and national burden of neurological disorders during 1990-2015: a systematic analysis for the global burden of disease study 2015. Lancet Neurol 16:877–897. https://doi.org/10.1016/S1474-4422(17)30299-5

Herrero-Herranz E, Pardo LA, Gold R, Linker RA (2008) Pattern of axonal injury in murine myelin oligodendrocyte glycoprotein induced experimental autoimmune encephalomyelitis: implications for multiple sclerosis. Neurobiol Dis 30:162–173. https://doi.org/10.1016/j.nbd.2008.01.001

Jasanoff A, Song S, Dinner AR, Wagner G, Wiley DC (1999) One of two unstructured domains of Ii becomes ordered in complexes with MHC class II molecules. Immunity 10:761–768

Karp DR, Teletski CL, Scholl P, Geha R, Long EO (1990) The alpha 1 domain of the HLA-DR molecule is essential for high-affinity binding of the toxic shock syndrome toxin-1. Nature 346:474–476. https://doi.org/10.1038/346474a0

Karp DR, Jenkins RN, Long EO (1992) Distinct binding sites on HLA-DR for invariant chain and staphylococcal enterotoxins. Proc Natl Acad Sci U S A 89:9657–9661

Kim J, Urban RG, Strominger JL, Wiley DC (1994) Toxic shock syndrome toxin-1 complexed with a class II major histocompatibility molecule HLA-DR1. Science 266:1870–1874

Leng L et al (2003) MIF signal transduction initiated by binding to CD74. J Exp Med 197:1467–1476. https://doi.org/10.1084/jem.20030286

Meza-Romero R et al (2014) HLA-DRalpha1 constructs block CD74 expression and MIF effects in experimental autoimmune encephalomyelitis. J Immunol 192:4164–4173. https://doi.org/10.4049/jimmunol.1303118

Meza-Romero R et al (2016a) Modeling of both shared and distinct interactions between MIF and its homologue D-DT with their common receptor CD74. Cytokine 88:62–70. https://doi.org/10.1016/j.cyto.2016.08.024

Meza-Romero R, Benedek G, Leng L, Bucala R, Vandenbark AA (2016b) Predicted structure of MIF/CD74 and RTL1000/CD74 complexes. Metab Brain Dis 31:249–255. https://doi.org/10.1007/s11011-016-9798-x

Niino M, Ogata A, Kikuchi S, Tashiro K, Nishihira J (2000) Macrophage migration inhibitory factor in the cerebrospinal fluid of patients with conventional and optic-spinal forms of multiple sclerosis and neuro-Behcet's disease. J Neurol Sci 179:127–131

Pos W, Sethi DK, Call MJ, Schulze MS, Anders AK, Pyrdol J, Wucherpfennig KW (2012) Crystal structure of the HLA-DM-HLA-DR1 complex defines mechanisms for rapid peptide selection. Cell 151:1557–1568. https://doi.org/10.1016/j.cell.2012.11.025

Powell ND, Papenfuss TL, McClain MA, Gienapp IE, Shawler TM, Satoskar AR, Whitacre CC (2005) Cutting edge: macrophage migration inhibitory factor is necessary for progression of experimental autoimmune encephalomyelitis. J Immunol 175:5611–5614

Reich DS, Lucchinetti CF, Calabresi PA (2018) Multiple Sclerosis. N Engl J Med 378:169–180. https://doi.org/10.1056/NEJMra1401483

Sospedra M, Martin R (2005) Immunology of multiple sclerosis. Annu Rev Immunol 23:683–747. https://doi.org/10.1146/annurev.immunol.23.021704.115707

Steinman L (1996) Multiple sclerosis: a coordinated immunological attack against myelin in the central nervous system. Cell 85:299–302

Vandenbark AA et al (2003) Recombinant TCR ligand induces tolerance to myelin oligodendrocyte glycoprotein 35-55 peptide and reverses clinical and histological signs of chronic experimental autoimmune encephalomyelitis in HLA-DR2 transgenic mice. J Immunol 171:127–133

Vandenbark AA et al (2013) A novel regulatory pathway for autoimmune disease: binding of partial MHC class II constructs to monocytes reduces CD74 expression and induces both specific and bystander T-cell tolerance. J Autoimmun 40:96–110. https://doi.org/10.1016/j.jaut.2012.08.004

Wingerchuk DM, Carter JL (2014) Multiple sclerosis: current and emerging disease-modifying therapies and treatment strategies. Mayo Clin Proc 89:225–240. https://doi.org/10.1016/j.mayocp.2013.11.002

Zamvil SS, Steinman L (1990) The T lymphocyte in experimental allergic encephalomyelitis. Annu Rev Immunol 8:579–621. https://doi.org/10.1146/annurev.iy.08.040190.003051